

Monodentate and bridging coordination of 2,5-dimercapto-1,3,4-thiadiazolate to a (2,2':6',2''-terpyridine)platinum(II) center †

Hidenori Tannai,^a Kiyoshi Tsuge,^{*a} Yoichi Sasaki,^{*a} Osamu Hatozaki^b and Noboru Oyama^b

^a Division of Chemistry, Graduate School of Science, Hokkaido University, Sapporo 060-0810, Japan. E-mail: yasaki@sci.hokudai.ac.jp

^b Department of Applied Chemistry, Faculty of Technology, Tokyo University of Agriculture and Technology, Naka-cho, Koganei, Tokyo 184-8588, Japan

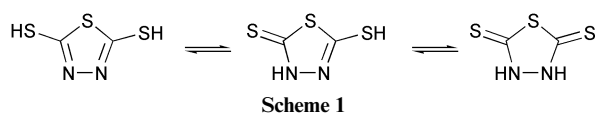
Received 4th February 2003, Accepted 16th April 2003

First published as an Advance Article on the web 7th May 2003

A series of mono- and di-nuclear platinum complexes, [Pt(trpy)(McMT)](PF₆) (**1**), [Pt(trpy)(DMcTH)](PF₆) (**2**) and [(Pt(trpy))₂(DMcT)](PF₆)₂ (**3**) have been synthesized by the reaction of [Pt(trpy)(OH)](PF₆) with mercapto- and dimercapto-thiadiazoles (trpy = 2,2':6',2''-terpyridine, McMTH = 2-mercapto-5-methyl-1,3,4-thiadiazole, DMcTH₂ = 2,5-dimercapto-1,3,4-thiadiazole). The X-ray structure determinations revealed that the mercaptothiadiazoles coordinate to the platinum centers as κ¹S-thiolate forms in all three complexes. Mononuclear DMcT–Pt complex **2** has a free thioamide group which is responsible for the formation of a hydrogen-bonded dimeric structure in the solid state. The complexes **1** and **2** show LLCT emissions in the solid state, whereas **3** is non-emissive. Cyclic voltammograms of the three complexes in DMF commonly show two reduction processes at *ca.* –0.7 V and –1.3 V based on the {Pt(trpy)}²⁺ units. Complex **2** further shows the oxidation of a free thioamide group at 0.32 V (*vs.* Ag/AgCl) on the addition of Et₃N.

Introduction

N-Heterocyclic thiones containing a thioamide group are intriguing ligands in coordination chemistry, since these ligands can achieve versatile coordination modes using exocyclic sulfur and endocyclic nitrogen atoms (Scheme 1).^{1–4} They show prototropic tautomerism, acid–base equilibrium, and redox reactions based on mercapto→disulfido conversion. Because of these features their coordination chemistry is amongst the most versatile. Not only transition metal but also non-transition metal complexes have been extensively studied with a variety of heterocyclic thiones having 5-membered, 6-membered and other condensed cycles.^{5–7} Among N-heterocyclic thiones, 2,5-dimercapto-1,3,4-thiadiazole (DMcTH₂) which is commonly known as bismuthiol I, is particularly interesting, since the five donor sites in its protonated and deprotonated forms enable coordination to two or more metal ions within a rather rigid and compact molecular space and interactions between metal ions may be promoted.^{8–13} Thus, DMcTH_n^{(2–n)–} (*n* = 0–2) is a useful ligand in the construction of multifunctional metal complexes. Moreover, DMcTH₂ is known as a useful cathode material in high performance lithium second batteries based on the redox reaction of its mercapto group.¹⁴ The interaction of DMcTH₂ with metal electrodes has been reported to play an important role in the redox reactions in the cell. Therefore, the redox chemistry of DMcTH₂ itself and also that on metal surfaces have been the subject of current extensive studies.^{15–19}



While the understanding of the redox chemistry of the metal complexes of DMcTH_n^{(2–n)–} should be important in these contexts, no structurally well defined metal complex, which is appropriate for redox studies, has been reported. Indeed, most DMcTH_n^{(2–n)–} complexes so far known are insoluble powders and thus their coordination modes remain ambiguous. Obviously, the ligand easily acts as a bridging ligand due to

its multidentate nature resulting in structural complication. X-Ray structural determinations of DMcT complexes so far available are those of two d¹⁰ metal complexes, [(MeHg)₂–(DMcT)]₂,²⁰ [(Me₂Tl)(DMcT)]₂,²¹ one organoruthenium complex, [Ru(PPh₃)₂(CO)(DMcTH)₂],²² and gold complexes with DMcT^{2–}.^{23,24} Although typical transition metal complexes with DMcTH_n^{(2–n)–} could provide important structural and redox characteristics associated with this versatile ligand, no such structurally determined complexes are available so far.

We have initiated the study of transition metal complexes of DMcTH_n^{(2–n)–} and its related ligands. As a first step, we have chosen platinum(II), which takes square planar geometry and therefore the steric hindrance among the ligands is minimized. With the cooperation of a tridentate ligand, 2,2':6',2''-terpyridine (trpy), the metal center leaves only one coordination site for the mercaptothiadiazole ligands, and structural complications arising from the multidentate nature of the ligand may be avoided. We have found that for the first time the dimercapto ligand takes both monodentate and bridging coordination modes with the same metal center. In this paper, we report the syntheses, structures and redox properties of a series of three mono- and di-nuclear platinum complexes having deprotonated forms of DMcTH₂ and its methyl congener, 2-mercapto-5-methyl-1,3,4-thiadiazole (McMTH).

Experimental

Materials

Ligands McMTH and DMcTH₂ were purchased from Tokyo Kasei and recrystallized before use. The platinum(II) starting complex [Pt(trpy)(OH)](PF₆) was prepared by following the literature method for the preparation of the corresponding BF₄[–] salt by using NH₄PF₆ instead of NaBF₄.²⁵

Syntheses

[Pt(trpy)(McMT)](PF₆) (1**).** An acetone suspension (10 ml) of [Pt(trpy)(OH)](PF₆) (118 mg, 0.20 mmol) was added to an acetone solution (20 ml) of McMTH (26.4 mg, 0.20 mmol) to obtain an orange solution. The slow evaporation of the solvent at room temperature resulted in the formation of red crystals. The crystals were collected by filtration and dried under vacuum (123 mg, 0.174 mmol, 87%) (Found: C, 30.72; H, 2.16;

† Electronic supplementary information (ESI) available: the UV-vis absorption spectra of **2** on the addition of Et₃N. See <http://www.rsc.org/suppdata/dt/b3/b301390c>

Table 1 Crystallographic data for **1**, **2** and **3**·2CH₃COCH₃

	1	2	3 ·2CH ₃ COCH ₃
Formula	C ₁₈ H ₁₄ N ₅ S ₂ F ₆ Pt	C ₁₇ H ₁₂ N ₅ S ₃ F ₆ Pt	C ₃₈ H ₃₄ N ₈ S ₃ F ₁₂ O ₂ P ₂ Pt ₂
<i>M</i>	704.52	722.55	1411.03
<i>T</i> /°C	23	−166	−153
Crystal system	Monoclinic	Triclinic	Triclinic
Space group	<i>P</i> 2 ₁ / <i>a</i>	<i>P</i> $\bar{1}$	<i>P</i> $\bar{1}$
<i>a</i> /Å	11.269(4)	10.771(2)	5.800(2)
<i>b</i> /Å	16.431(5)	11.599(3)	13.071(1)
<i>c</i> /Å	11.775(5)	9.660(1)	14.879(3)
<i>a</i> /°	90	99.05(1)	94.517(5)
<i>β</i> /°	92.19(1)	112.84(1)	91.111(2)
<i>γ</i> /°	90	104.80(1)	97.789(2)
<i>V</i> /Å ³	2178(1)	1029.8(3)	1113.7(4)
<i>Z</i>	4	2	1
<i>μ</i> /mm ^{−1}	6.749	7.239	6.558
<i>d</i> _{calcd} /g cm ^{−3}	2.15	2.33	2.10
No. of unique reflns (<i>R</i> _{int})	4483 (0.036)	4476 (0.078)	4567 (0.019)
No. of obsd reflns	3995, <i>I</i> > 2σ(<i>I</i>)	3985, <i>I</i> > 2σ(<i>I</i>)	4058, <i>I</i> > 2σ(<i>I</i>)
<i>R</i> 1, <i>wR</i> 2 ^a	0.057, 0.146	0.056, 0.143	0.027, 0.053

$$^a R1 = \sum ||F_o| - |F_c|| / \sum |F_o|, wR2 = \{ \sum [w(F_o^2 - F_c^2)^2] / \sum [w(F_o^2)] \}^{1/2} \text{ with } w = \{ \sigma^2(F_o^2) + [x(\max(F_o^2, 0) + 2F_c^2)/3] \}^{-1}.$$

N, 10.14; S, 9.26. C₁₈H₁₄N₅S₂F₆Pt requires C, 30.69; H, 2.00; N, 9.94; S, 9.10%; δ_H (solvent CD₃CN) 2.50 (3H, s), 7.74 (2H, t), 8.32 (5H, m), 8.46 (2H, t), 9.11 (2H, d).

[Pt(trpy)(DMcTH)](PF₆) (2). An acetone suspension (10 ml) of [Pt(trpy)(OH)](PF₆) (118 mg, 0.20 mmol) was added to an acetone solution (20 ml) of DMcTH₂ (30.1 mg, 0.20 mmol), to obtain an orange solution. Diffusion of diethyl ether into the orange solution led to the formation of red crystals, which were collected by filtration and dried under vacuum (113 mg, 0.156 mmol, 78%) (Found: C, 28.34; H, 1.75; N, 9.67; S, 13.26. C₁₇H₁₂N₅S₃F₆Pt requires C, 28.26; H, 1.67; N, 9.69; S, 13.31%; δ_H (solvent CD₃CN) 7.82 (2H, t), 8.38 (5H, m), 8.49 (2H, t), 9.16 (2H, d), 11.5 (1H, s).

[Pt(trpy)₂(DMcT)](PF₆)₂ (3). An acetone suspension (10 ml) of [Pt(trpy)(OH)](PF₆) (59 mg, 0.10 mmol) was added to an acetone solution (110 ml) of DMcTH₂ (7.5 mg, 0.05 mmol), to obtain a red purple solution. Diffusion of diethyl ether into the solution resulted in the formation of red crystals. The crystals were collected by filtration and dried under vacuum (58 mg, 0.044 mmol, 88%) (Found: C, 29.46; H, 1.91; N, 8.46; S, 7.41. C₃₂H₂₂N₈S₃F₁₂P₂Pt₂ requires C, 29.68; H, 1.71; N, 8.65; S, 7.43%; δ_H (solvent DMSO-*d*₆) 7.88 (4H, t), 8.49 (4H, t), 8.66 (10H, m), 9.02 (4H, d). The red crystals initially contain two acetone molecules per one complex cation as crystal solvent, which were slowly released at room temperature and completely removed under vacuum.

Physical measurements

UV-vis spectra were taken on a Hitachi U-3410 spectrophotometer. Emission spectra were measured by the use of a Hitachi F-4500 spectrophotometer. ¹H-NMR spectra were obtained on a JEOL JNM-EX 270 NMR spectrometer at 270 MHz. Cyclic voltammograms were obtained by using a Hokuto HZ-3000 system. The working, auxiliary and reference electrodes were platinum electrode, platinum wire, and Ag/AgCl, respectively. All the electrochemical measurements were performed under an Ar atmosphere in DMF solutions containing 0.1 M tetra-*n*-butylammonium hexafluorophosphate, with a complex concentration of 0.5 mM.

X-Ray diffraction studies

Suitable crystals of **1**, **2** and **3**·2CH₃COCH₃ were obtained from acetone solutions as described in the Syntheses section. The selected crystals were mounted onto a thin glass fiber. Measurements on **1** and **3**·2CH₃COCH₃ were made on a Mercury

CCD area detector coupled with a Rigaku AFC-8S diffractometer with graphite-monochromated Mo-*K*α radiation. Final cell parameters were obtained from a least-squares analysis of reflections with *I* > 10σ(*I*). Space groups were determined on the basis of systematic absences, a statistical analysis of intensity distribution, and the successful solution and refinement of the structures. Data were collected at temperatures of 23 and −153 °C for **1** and **3**·2CH₃COCH₃, respectively, to a maximum 2θ value of 55°. Data were collected in 0.5° oscillations (in ω) with 120.0 s exposures (in two 60.0 s repeats to allow dezingering). Sweeps of data were done using ω oscillations for −76 to 114° at χ = 45.0° and φ = 0.0° and from −16 to 44° at χ = 45.0° and φ = 90.0°. The crystal-to-detector distance was 40.0 mm, and the detector swing angle was 14.0°. Data were collected and processed using Crystal Clear.²⁶ An empirical absorption correction resulted in acceptable transmission factors. The data were corrected for Lorentz and polarization factors.

Measurement of **2** was made on a RIGAKU RAXIS-RAPID diffractometer with an imaging plate area detector using graphite-monochromated Mo-*K*α radiation at −166 °C. To determine the cell constants and the orientation matrix, two oscillation photographs were taken with an oscillation angle of 5°. Intensity data were collected by taking oscillation photographs (total oscillation range were 220°, 44 frames, and exposure time 180 s per degree). A numerical absorption correction was applied. The data were corrected for Lorentz and polarization factors.

All the calculations were carried out on a Silicon Graphics O2 computer system using TEXSAN.²⁷ The structures were solved by direct methods and expanded using Fourier and difference Fourier techniques. The DMcT^{2−} was disordered in structure **3**, since DMcT^{2−} was located near the inversion center. When the space group was assumed to be *P*1, the disorder remained and the *R* value did not improve. Therefore, the space group for the crystal of **3**·2CH₃COCH₃ was determined as *P* $\bar{1}$. Details of crystal parameters and structure refinement are given in Table 1. Selected bond lengths and angles are shown in Table 2.

CCDC reference numbers 203194–203196.

See <http://www.rsc.org/suppdata/dt/b3/b301390c/> for crystallographic data in CIF or other electronic format.

Results and discussion

Synthesis

We have used a {Pt(trpy)} unit for coordination of McMT[−] and DMcTH_{*n*}^{(2−*n*)−} (*n* = 1, 2). The ligands tend to give polymerized

Table 2 Selected bond distances (Å) and angles (°) for **1**, **2**, and **3**·2CH₃COCH₃

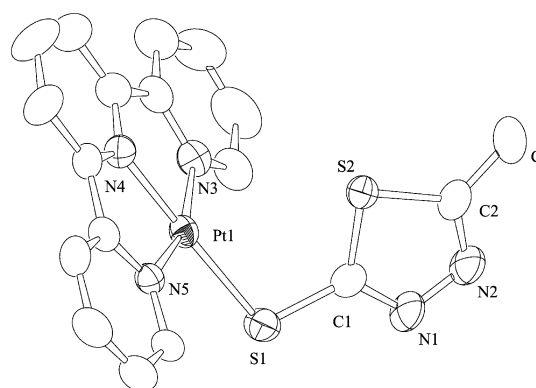
1			
Pt–S1	2.308(2)	S1–Pt–N3	100.7(2)
Pt–N3	2.028(5)	S1–Pt–N5	98.3(1)
Pt–N4	1.954(7)	N3–Pt–N4	79.8(3)
Pt–N5	2.035(5)	N4–Pt–N5	81.3(2)
S1–C1	1.752(7)	Pt–S1–C1	102.4(2)
2			
Pt–S1	2.313(2)	S1–Pt–N3	100.0(2)
Pt–N3	2.020(9)	S1–Pt–N5	97.3(2)
Pt–N4	1.945(7)	N3–Pt–N4	80.9(4)
Pt–N5	2.009(9)	N4–Pt–N5	81.8(3)
S1–C1	1.75(1)	Pt–S1–C1	105.2(3)
S3–C2	1.64(1)		
3 ·2CH ₃ COCH ₃			
Pt–S1	2.306(1)	S1–Pt–N3	99.4(1)
Pt–N3	2.015(4)	S1–Pt–N5	98.4(1)
Pt–N4	1.970(3)	N3–Pt–N4	81.1(1)
Pt–N5	2.023(4)	N4–Pt–N5	81.2(1)

species when a metal center has two or more available coordination sites. The {Pt(trpy)} unit with only one free coordination site has successfully provided a series of three discrete complexes **1**, **2** and **3** in quite high yields. The reactions between [Pt(trpy)(OH)](PF₆) and these ligands proceeded smoothly at ambient temperature, although the platinum(II) center is generally regarded as a substitution inert metal center. The short reaction time found in the formation of **1**, **2**, and **3** is in sharp contrast to, for example, the case of the preparation of the Pt–trpy complexes of pyrimidinethiol and dithiouracil that required reflux of the reaction mixture of [Pt(trpy)Cl]⁺ and corresponding sodium thiolates in MeOH for *ca.* 12 h.²⁸ The basic hydroxo complex has now been proved to be a much better platinum source for the reaction with the acidic mercaptothiadiazole ligands. It appears that the transfer of the proton from the ligand to the coordinated hydroxo group facilitates the substitution of the anionic ligand for the easily replaceable H₂O.

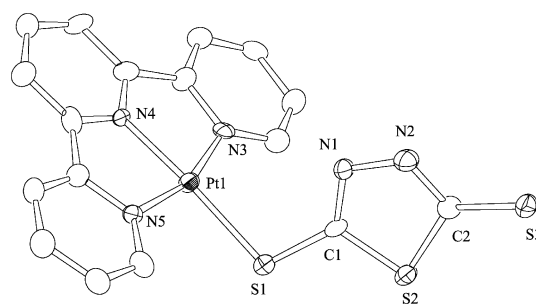
For the dimercapto ligand DMcTH_n^{(2–n)–}, both monomeric and dimeric complexes with monodentate and bridging ligands, respectively, have been prepared. The nuclearity of the product has been controlled simply by the ratio of [Pt(trpy)(OH)](PF₆) to DMcTH₂. With one and two equivalent amounts of platinum complex to the ligand, the monomeric and dimeric complexes, respectively, have been obtained. The dimeric complex has also been prepared by stepwise reactions. Thus the addition of one equivalent amount of [Pt(trpy)(OH)](PF₆) to **2** has led to the formation of the dimeric complex **3**. In all these new complexes, the ligands coordinate to the platinum center *via* a sulfur donor site (*vide infra*), suggesting the soft nature of the {Pt–trpy} unit, being consistent with the coordination mode of the pyrimidinethiolate and dithiouracilate ligands to the {Pt–trpy} moiety.²⁸

Structures

The X-ray structure analyses have been performed on the three complexes. Fig. 1 shows the ORTEP²⁹ drawing of McMT complex **1**. The square planar platinum atom is coordinated by three nitrogen atoms of trpy and a sulfur atom of McMT[–]. The two planar ligands, trpy and McMT[–], are not in the same plane. Ligand McMT[–] coordinates to the metal center in the thiolate form rather than the thione form. The Pt–S1 distance is comparable to those of analogous pyridine- and pyrimidine-thiol Pt complexes (Pt–S: 2.29–2.31 Å).²⁸ The other sulfur atom S2 is separated from Pt by 3.30 Å which is long enough to neglect any bonding interaction. The intermolecular Pt–Pt distance (4.92 Å) indicates no strong interaction between Pt atoms.

**Fig. 1** ORTEP plot of the structure of the complex cation [Pt(trpy)-(McMT)]⁺ with 50% probability ellipsoids.

As shown in Fig. 2, mononuclear DMcT complex **2** has a very similar structure to that of McMT complex **1**. The ligand should be in a monoanionic form DMcTH[–] as concluded from the detailed ligand structure as given below as well as the expected chemical formula. The ligand coordinates to the platinum atom with one of the thiolate sulfurs. The second nearest donor site of the ligand to Pt is N1. The long distance between Pt and N1 of 3.36 Å indicates, however, no bonding interaction between them. It is noted that the S–C distance of the coordinated mercapto group is longer than that of the free mercapto group (S1–C1: 1.75 Å, S3–C2: 1.64 Å). The difference in the S–C distances provides some information on the ligand tautomerism. It is well known that the S–C distances in the thiol form are in the range 1.65 Å to 1.70 Å.¹ Therefore, the coordinated mercapto group in **2** is in the thiol form, whereas the free mercapto group is in the thione form. In the difference Fourier map, electron density corresponding to a hydrogen atom was found on N2 and not on N1, which is consistent with the suggested thiol–thione form of DMcT[–]. Fig. 3 shows hydrogen bonded coupling between the two complex cations through the thioamide hydrogen. The coupled dimer units are further piled up with π – π stacking of {Pt(trpy)} units.

**Fig. 2** ORTEP plot of the structure of the complex cation [Pt(trpy)-(DMcTH)]⁺ with 50% probability ellipsoids.

The ¹H-NMR spectrum of complex **2** in acetonitrile solution shows a characteristic signal at δ = 11.5 ppm. It has been reported that thioamido forms are generally featured by the signals around 8–11 ppm, while thiol forms are characterised by the signals around 3–4 ppm.¹ It is thus concluded that the thioamide form in **2** is intact also in solution.

In the crystal of dinuclear complex **3**, the doubly deprotonated DMcT^{2–} ligand bridges between the two platinum units. The crystallographically imposed inversion center manifests the disorder of the DMcT^{2–} ligand over two positions, which precludes a detailed discussion of bond lengths in the DMcT^{2–} ligand. For clarity, one set of DMcT^{2–} ligands is shown in Fig. 4. Since this molecule has an inversion center, two {Pt(trpy)} moieties are parallel to each other.

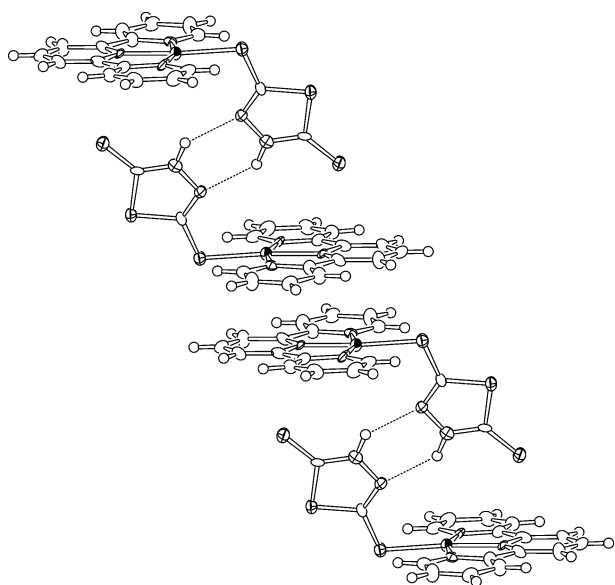


Fig. 3 Hydrogen bonds of **2** in the crystal structure.

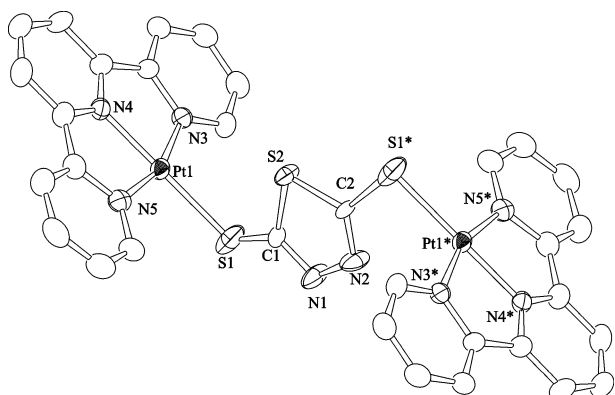


Fig. 4 ORTEP plot of the structure of the complex cation $[(\text{Pt}(\text{trpy}))_2(\text{DMcT})]^{2+}$ with 50% probability ellipsoids. Symmetry code: * $-x, -y, -z$.

The structural features of the present Pt complexes may be compared with those of other $\text{DMcTH}_n^{(2-m)-}$ complexes. The complexes whose structures are reported include one ruthenium,²² one mercury,²⁰ one thallium²¹ and gold complexes.^{23,24} The thallium complex is not a discrete complex but a solid state polymer constructed mainly of ionic interactions between $\{\text{Tl}(\text{Me})_2\}^+$ and DMcT^{2-} ($\text{Tl} \cdots \text{S} > 3.2 \text{ \AA}$, $\text{Tl} \cdots \text{N} > 2.7 \text{ \AA}$), and DMcT^{2-} may be regarded as a counter anion rather than a ligand. The mercury, gold and ruthenium complexes are molecular complexes, in which the DMcT^{2-} ligand coordinates to the metal center *via* the thiolate sulfur atoms. The mercury and gold complexes take dinuclear structures bridged by dianionic DMcT^{2-} , similar to the platinum dinuclear complex **3**. The ruthenium complex is a mononuclear complex having two monoanionic DMcTH^- ligands, one of which coordinates to the ruthenium atom in an N,S-chelate form and the other in a monodentate thiolate form. Despite the difference in coordination modes, both DMcTH^- ligands in the ruthenium complex have free mercapto groups in the thioamide forms, the same as that in the mononuclear platinum complex **2**. It should be noted that both mono- and di-nuclear DMcT complexes have been synthesized and structurally characterized for the first time with a single metal center $\{\text{Pt}(\text{trpy})\}$ unit. The stepwise introduction of the platinum centers into the $\text{DMcTH}_n^{(2-m)-}$ ligand indicates its potential usage as a building unit for designed heterometallic complexes. Heterometallic complexes thus obtained in this laboratory will be reported elsewhere.

UV-vis and emission spectra

The UV-vis absorption spectra of **1**, **2** and **3** are shown in Fig. 5. All the complexes show strong bands in the region $< 350 \text{ nm}$, shoulders in the region $350\text{--}400 \text{ nm}$ and weak broad bands around 500 nm . Terpyridine ligands in various platinum(II) complexes are known to show strong intra-ligand $\pi\text{--}\pi^*$ transitions at $< 350 \text{ nm}$ with vibronic structures.^{28,30–35} Since such vibronic structure is also observed in the spectra of **1** and **3**, the absorption in this region should be originated mainly from the terpyridine ligand. The characteristic vibronic feature is not clearly seen in the spectrum of **2**. The vibronic structure has been recovered, however, on addition of triethylamine (Fig. S1†), which should cause the deprotonation of the DMcTH^- ligand to give DMcT^{2-} . It may be that the N-protonated thioamide form of DMcTH^- possesses some absorption in the region $< 350 \text{ nm}$. Such absorption would disappear on deprotonation and/or coordination by a sulfur atom. According to previous papers, the absorption bands of Pt–trpy complexes in the visible region are attributed to metal-to-ligand (ML),^{25,31–33,35} or ligand-to-ligand (LL)^{28,34} charge transfer (CT) transitions. The shoulders in the region $350\text{--}400 \text{ nm}$ of the present complexes may be assigned to MLCT transitions within the $\{\text{Pt}(\text{trpy})\}$ unit.^{25,35} We have assigned the weak broad band around 500 nm to a LLCT transition from S(p) (thiadiazole ligand) to $\pi^*(\text{trpy})$, by considering the following. The LLCT absorptions are common to Pt–bipyridine and –phenanthroline complexes with thiol ligands, since the relatively high lying S(p) orbital and only slightly higher π^* orbital of the diimine ligands are involved.^{36–40} The Pt–trpy complexes with aromatic thiols such as pyridinethiol, pyrimidinethiol and pyrimidinedithiol (dithiouracil), also exhibit LLCT bands around 500 nm (λ_{max} : $482\text{--}520 \text{ nm}$; ϵ : $\approx 10^3 \text{ mol cm}^{-1}$).²⁸

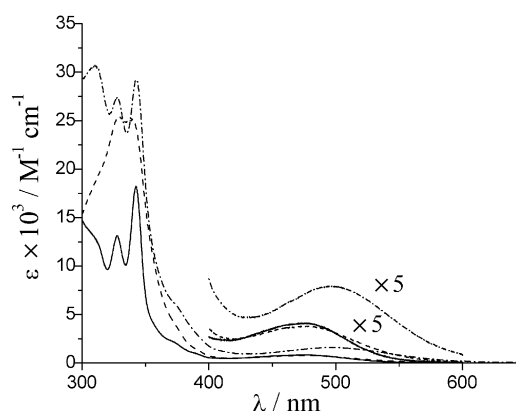


Fig. 5 UV-vis absorption spectra of **1** (—), **2** (---) and **3** (-.-) in CH_3CN .

The luminescent properties of the new complexes have been studied briefly, since the $\{\text{Pt}(\text{trpy})\}$ unit is well known as a photochemically active center that shows various types of emission such as intra-ligand, MLCT, MMLCT or LLCT emissions depending on the ancillary ligands.^{25,28,31–33,35,36,41,42} The emission spectra of powdered samples of **1**, **2** and **3** have been measured at room temperature. As shown in Fig. 6, monomeric complexes **1** and **2** show emission maxima at 620 nm and 607 nm , respectively, while dimeric complex **3** does not show any emission. The luminescence properties of platinum terpyridine complexes with the aromatic thiols mentioned above have been reported to show emission bands in the region from 640 to 710 nm in solution. These emissions were considered as being of the LLCT type.²⁸ From the similarity of absorption and emission energies among hitherto reported complexes and present complexes **1** and **2**, we have concluded that the emissions of the present complexes are associated with the LLCT excited state. It is interesting that dimeric complex **3**

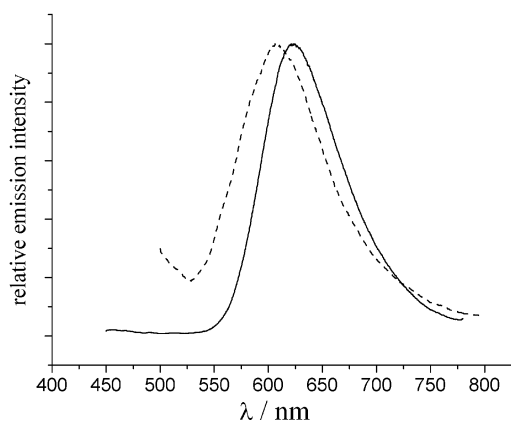


Fig. 6 Emission spectra of powdered samples of **1** (—) and **2** (---) at room temperature with $\lambda_{\text{ex}} = 400$ nm and $\lambda_{\text{ex}} = 450$ nm, respectively.

is non-emissive. It may be that there is some kind of interaction between the two $\{\text{Pt}(\text{trpy})\}$ units through the bridging ligand to produce some quenching pathways.

The nearest Pt \cdots Pt distances in the crystal of complexes **1** and **2** are too long (4.916(1) Å and 4.619(1) Å, respectively) to perturb the excited state effectively as observed for other Pt(trpy) complexes.^{31–33,36,41,43} The distances between the neighboring $\{\text{Pt}(\text{trpy})\}$ planes are 3.35 Å and 3.52 Å for **1** and **2**, respectively, which are within the range which can cause excimer interaction,^{31,43,44} however.

Cyclic voltammetry

Fig. 7 shows the CV of **1**, **2** and **3** in DMF solution. In common to all three complexes, there are two redox waves at *ca.* -0.7 V and -1.3 V vs. Ag/AgCl. It has been reported that Pt-trpy complexes with an ancillary ligand show redox couples around -0.6 and -1.2 V corresponding to the reduction of the terpyridine ligand.³⁰ Since McMT^- , DMcTH^- and DMcT^{2-} are not reduced in the range from 0 V to -2 V,^{15–17} the observed redox waves should be based on the reductions of the terpyridine ligands. The two redox waves of dinuclear complex **3** do not show any sign of splitting indicating that

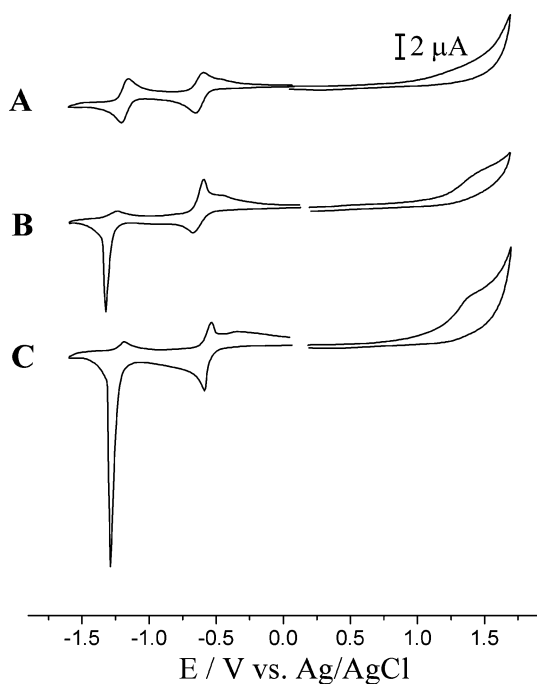


Fig. 7 Cyclic voltammograms of 0.5 mM solution of **1**, **2** and **3** in 0.1 M $[(n\text{-Bu}_4)\text{N}][\text{PF}_6]/\text{DMF}$ with a platinum working electrode at a scan rate of 100 mV s^{-1} . (A): **1**; (B): **2**; (C): **3**.

the redox interaction between the two $\{\text{Pt-trpy}\}$ units is small. Platinum(II) which has fully occupied d_π orbitals would not provide an effective pathway for the electron-exchange. Moreover, the LUMO of the bridging DMcT^{2-} should be much higher in energy and therefore would make favourable π interactions difficult. The perpendicular arrangement of trpy and DMcT^{2-} could be also relevant to the absence of redox interactions.

Complex **2** has one free mercapto group on the thiadiazole ligand. Although the complex does not show any oxidation wave in the region studied, an irreversible oxidation wave appears at $E_{\text{pa}} = +0.32$ V on addition of the base (Fig. 8). The wave disappears again on addition of acid (*p*-toluenesulfonic acid). Thus the irreversible oxidation wave at $+0.32$ V corresponds to the oxidative coupling of the free thiolate groups. The proton coupled redox behavior of **2** is summarized in Scheme 2. The oxidation of the thiolate group of the free ligands DMcTH^- and DMcT^{2-} was observed at 0.2 V and 0.1 V, respectively.¹⁵ It is seen therefore that coordination of $\text{DMcTH}_n^{(2-n)-}$ to a metal center causes significant influence of the redox potential on the thiolate–dithiol redox process. This is the first time that the redox reactions of the free end of coordinated DMcT have been observed.

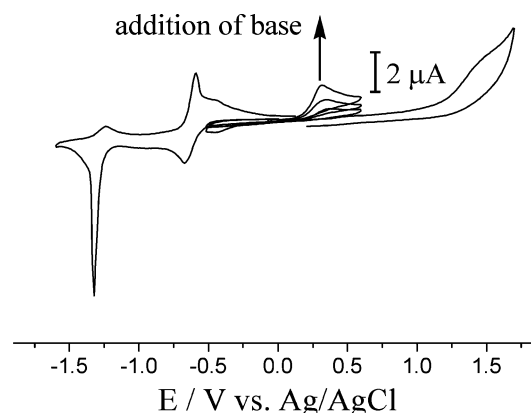
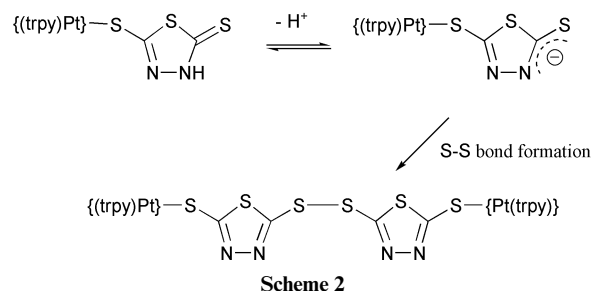


Fig. 8 Cyclic voltammograms of **2** on the addition of Et_3N . The irreversible oxidation wave corresponding to the oxidation of the thiolate group appeared at 0.32 V.



Conclusion

A series of mono- and di-nuclear $\text{DMcTH}_n^{(2-n)-}$ ($n = 0, 1$) and McMT^- complexes have been prepared for the first time with a single metal center, $\{\text{Pt}(\text{trpy})\}$. Structural studies revealed that while the Pt is coordinated at thiolate sulfur, the proton of the monodentate DMcTH^- resides on endocyclic nitrogen, suggesting typical soft character of the $\{\text{Pt}(\text{trpy})\}$ unit. While the redox processes of the two $\{\text{Pt}(\text{trpy})\}$ units in **3** are non-interactive (no splitting of the redox wave), disappearance of the photoluminescence on dimer formation indicates some interactions between the two units. The stepwise introduction of $\{\text{Pt}(\text{trpy})\}$ units to a DMcT ligand indicates that the mononuclear DMcT complex **2** is useful for the construction of heterodimeric and oligomeric complexes based on the compact bridging ligand.

Acknowledgements

This work is partly supported by a Grant-in-Aid for Encouragement of Young Scientists No. 13740367 from Japan Society for the Promotion of Science.

References

- 1 E. S. Raper, *Coord. Chem. Rev.*, 1985, **61**, 115.
- 2 E. S. Raper, *Coord. Chem. Rev.*, 1994, **129**, 91.
- 3 E. S. Raper, *Coord. Chem. Rev.*, 1996, **153**, 199.
- 4 E. S. Raper, *Coord. Chem. Rev.*, 1997, **165**, 475.
- 5 K. Umakoshi and Y. Sasaki, *Adv. Inorg. Chem.*, 1994, **40**, 187.
- 6 (a) K. Umakoshi, T. Yamasaki, A. Fukuoka, H. Kawano and M. Ichimura, *Inorg. Chem.*, 2002, **41**, 4093; (b) O. Asada, K. Umakoshi, K. Tsuge, S. Yabuuchi, Y. Sasaki and M. Onishi, *Bull. Chem. Soc. Jpn.*, 2003, **76**, 549.
- 7 P. D. Akrivos, *Coord. Chem. Rev.*, 2001, **213**, 181.
- 8 S. A. A. Zaidi, A. S. Farooqi, D. K. Varshney, V. Islam and K. S. Siddiqi, *J. Inorg. Nucl. Chem.*, 1977, **39**, 581.
- 9 M. Brezeanu, R. Olar, A. Meghea, N. Stanica and C. T. Supuran, *Rev. Roum. Chim.*, 1996, **41**, 103.
- 10 M. R. Gajendragad and U. Agarwala, *Z. Anorg. Allg. Chem.*, 1975, **415**, 84.
- 11 P. Ortega, L. R. Ver and M. E. Guzmán, *Macromol. Chem. Phys.*, 1997, **198**, 2949.
- 12 S. A. A. Zaidi and D. K. Varshney, *J. Inorg. Nucl. Chem.*, 1975, **37**, 1804.
- 13 M. R. Gajendragad and U. Agarwala, *Indian J. Chem.*, 1975, **13**, 697.
- 14 N. Oyama, T. Tatsuma, T. Sato and T. Sotomura, *Nature (London)*, 1995, **373**, 598.
- 15 E. Shouji, Y. Yokoyama, J. M. Pope, N. Oyama and D. A. Buttry, *J. Phys. Chem. B*, 1997, **101**, 2861.
- 16 T. Tatsuma, H. Matsui, E. Shouji and N. Oyama, *J. Phys. Chem.*, 1996, **100**, 14016.
- 17 E. Shouji and D. A. Buttry, *J. Phys. Chem. B*, 1999, **103**, 2239.
- 18 F. Matsumoto, M. Ozaki, Y. Inatomi, S. C. Paulson and N. Oyama, *Langmuir*, 1999, **15**, 857.
- 19 L. Huang, F. Tang, B. Hu, J. Shen, T. Yu and Q. Meng, *J. Phys. Chem. B*, 2001, **105**, 7984.
- 20 M. V. Castaño, M. M. Pasencia, A. Maciasas, J. S. Casas, J. Sordo and E. E. Castellano, *J. Chem. Soc., Dalton Trans.*, 1989, 1409.
- 21 M. V. Castaño, A. Sanches, J. S. Casas, J. Sordo and E. E. Castellano, *Inorg. Chim. Acta*, 1992, **201**, 83.
- 22 P. Mura, B. G. Olby and S. D. Robinson, *Inorg. Chim. Acta*, 1985, **97**, 45.
- 23 J. D. E. T. Wilton-Ely, A. Shier and H. Schmidbaur, *Organometallics*, 2001, **20**, 1895.
- 24 J. D. E. T. Wilton-Ely, A. Schier, N. W. Mitzel and H. Schmidbaur, *Inorg. Chem.*, 2001, **40**, 6266.
- 25 T. K. Aldridge, E. M. Stacy and D. R. McMillin, *Inorg. Chem.*, 1994, **33**, 722.
- 26 Crystal Clear, Rigaku Corp., Tokyo, 1999.
- 27 TEXSAN, Crystal Structure Analysis Package, Molecular Structure Corporation, Houston, TX, 1992.
- 28 B.-C. Tzeng, W.-F. Fu, C.-M. Che, H.-Y. Chao, K.-K. Cheung and S.-M. Peng, *J. Chem. Soc., Dalton Trans.*, 1999, 1017.
- 29 M. N. Burnett and C. K. Johnson, ORTEP-III: Oak Ridge Thermal Ellipsoid Plot Program for Crystal Structure Illustrations, Report ORNL-6895, Oak Ridge National Laboratory, Oak Ridge, TN, USA, 1996.
- 30 M. G. Hill, J. A. Bailey, V. M. Miskowski and H. B. Gray, *Inorg. Chem.*, 1996, **35**, 4585.
- 31 J. S. Field, R. J. Haines, D. R. McMillin and G. C. Summerton, *J. Chem. Soc., Dalton Trans.*, 2002, 1369.
- 32 V. W.-W. Yam, R. P.-L. Tang, K. M.-C. Wong and K.-K. Cheung, *Organometallics*, 2001, **20**, 4476.
- 33 S.-W. Lai, M. C. W. Chan, K.-K. Cheung and C.-M. Che, *Inorg. Chem.*, 1999, **38**, 4262.
- 34 V. W.-W. Yam, R. P.-L. Tang, K. M.-C. Wong, C.-C. Ko and K.-K. Cheung, *Inorg. Chem.*, 2001, **40**, 571.
- 35 H.-K. Yip, L.-K. Cheng, K.-K. Cheung and C.-M. Che, *J. Chem. Soc., Dalton Trans.*, 1993, 2.
- 36 V. W.-W. Yam, K. M.-C. Wong and N. Zhu, *J. Am. Chem. Soc.*, 2002, **124**, 6506.
- 37 S. D. Comings and R. Eisenberg, *J. Am. Chem. Soc.*, 1996, **118**, 1949.
- 38 S. D. Comings and R. Eisenberg, *Inorg. Chem.*, 1995, **34**, 2007.
- 39 J. M. Bevilacqua and R. Eisenberg, *Inorg. Chem.*, 1994, **33**, 1886.
- 40 J. A. Zuleta, J. M. Bevilacqua, D. M. Proserpio, P. D. Harvey and R. Eisenberg, *Inorg. Chem.*, 1992, **31**, 2396.
- 41 R. Buchner, J. S. Field, R. J. Haines, C. T. Cunningham and D. R. McMillin, *Inorg. Chem.*, 1997, **36**, 3952.
- 42 M. Akiba, K. Umakoshi and Y. Sasaki, *Chem. Lett.*, 1995, 607.
- 43 J. A. Bailey, M. G. Hill, R. E. Marsh, V. M. Miskowski, E. P. Schaefer and H. B. Gray, *Inorg. Chem.*, 1995, **34**, 4591.
- 44 V. M. Miskowski and V. H. Houlding, *Inorg. Chem.*, 1989, **28**, 1529.